AIAA 80-0670R

Higher Harmonic Control for Helicopters with Two-Bladed and Four-Bladed Rotors

Jing G. Yen*
Bell Helicopter Textron, Fort Worth, Texas

Theoretical investigations have been conducted to compare higher-harmonic blade pitch requirements for vibration reduction on helicopters with two-bladed teetering and four-bladed hingeless rotors in trimmed level flight. For the two-bladed teetering rotor, elimination of oscillatory two-per-rev (2*P*) hub vertical shear was studied. For the four-bladed hingeless rotor, higher-harmonic control (HHC) was used to minimize four-per-rev (4*P*) hub vertical shear, and rolling and pitching moments. Certain penalties in pitch-link loads and performance were predicted using higher-harmonic blade feathering. The penalties seem to be more serious for a two-bladed teetering rotor than those for a four-bladed hingeless rotor. A predictive algorithm for multiple inputs and multiple outputs was studied briefly and the nonlinear characteristics were discussed. Analytical results also indicate that both amplitude and phase of HHC vary significantly with airspeed for the four-bladed hingeless rotor. For the two-bladed teetering rotor, the required pitch amplitude increases as airspeed increases with nearly invariant phase angle.

Nomenclature

A_1	= lateral cyclic
B_1	= longitudinal cyclic
C_T	= thrust coefficient = $(T/\pi R^2\rho(R\Omega)^2)$
F	= 4/rev hub vertical shear
g	= load factor
PM	= 4/rev hub pitching moment
R	= rotor radius
RM	= 4/rev hub rolling moment
T	= rotor thrust force
$[T]$	= transfer matrix relating higher-harmonic control inputs to hub responses
$[T]^{-1}$	= inverse of transfer matrix
t	= time
t_c	= thrust coefficient = $2C_T/\sigma$
Δ	= indicates a perturbation quantity
θ	= blade collective
θ_0	= feathering amplitude
μ	= advance ratio
ρ	= air density
σ	= rotor solidity
ψ	= blade azimuth angle = Ωt
Ω	= rotor speed

Subscripts

c	= cosine component
i	= the ith blade
s	= sine component

Introduction

THE useful maximum speed of helicopters is frequently limited by vibration. For a two-bladed teetering rotor, the primary source of vibration is the two-per-rev (2*P*) hub shears. For a four-bladed hingeless rotor, the large four-per-rev (4*P*) hub moment plays as significant a role in vibration as the 4*P* hub shears. Numerous studies have been conducted in the past two decades to investigate the feasibility of using higher-harmonic blade pitch to reduce hub shears and moments transmitted to the fuselage by the rotor. Flight testing,[1] theoretical analysis,[2-5] and wind tunnel testing[6-10] have shown that higher-harmonic control (HHC) has the potential of minimizing airframe vibration levels by superposition of higher-harmonic blade feathering on the basic 1*P* cyclic pitch required by helicopter trim. The only flight test investigation of HHC for vibration reduction to date was conducted on a two-bladed teetering rotor in 1962 described in Ref. 1. The most recent studies have dealt with four-bladed articulated or hingeless rotors, with emphasis on wind tunnel testing (Refs. 8-10), and solution techniques to calculate both amplitude and phase of the HHC input required for attenuation of multiple oscillatory forces and moments (Refs. 11 and 12).

This paper uses a state-of-the-art helicopter simulation analysis to compare higher-harmonic blade pitch requirements on vibration reduction for helicopters with two-bladed teetering and four-bladed hingeless rotors in trimmed level flight. The objective is twofold: first, to exercise the analytical capability; second, to compare advantage and disadvantages of using HHC on a two-bladed teetering with those on a four-bladed hingeless rotor.

Two-Bladed Teetering Rotor HHC

Description of Math Model

Calculations were made with the Global Flight Simulation Program C81.[13] The rotor was modeled using four collective and five cyclic fully coupled modes generated by the Bell Helicopter Textron (BHT) Myklestad analysis.[14] The first collective torsion mode has a frequency of 2.92/rev. Pylon dynamics were represented in the rotor modes using hub impedance values, HSOFT and VSOFT,[14] a proven approach for calculation of rotor loads for teetering rotors. The BUNS unsteady aerodynamics option was used. Inputs defining fuselage dynamics and aerodynamics were supplied for a complete representation of the rotorcraft in free flight. C81 has the capability of harmonically varying blade pitch in either the fixed or the rotating system. Harmonic pitch can be obtained using collective, longitudinal cyclic, lateral cyclic, and cyclic stir in the fixed system or blade pitch excitation in the rotating frame. HHC can be implemented individually or simultaneously with maximum three shakers as limited by the current analytical capability.

2/rev Collective Pitch

For a two-bladed teetering rotor, the primary source of fuselage vibration is the 2*P* hub shears. Of these shears, the most costly to isolate, weightwise, is the 2*P* vertical shear. An

Presented as Paper 80-0670 at the AIAA/ASME/ASCE/AHS 21st Structures, Structural Dynamics and Materials Conference, Seattle, Wash., May 12-14, 1980; submitted June 16, 1980; revision received June 15, 1981.

*Chief Scientist—Flight Technology. Associate Fellow AIAA.

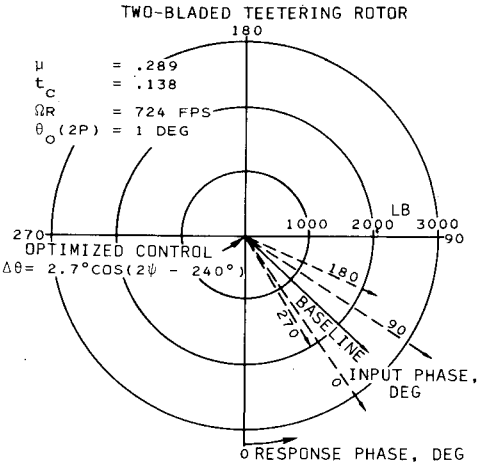

Fig. 1 Variation of 2*P* hub vertical shear with 2*P* collective input phase.

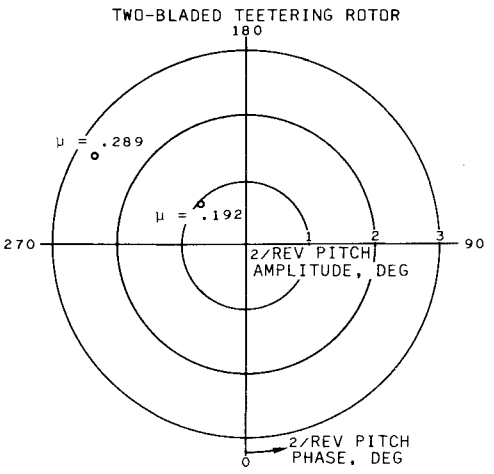

Fig. 2 Effect of advance ratio on 2*P* pitch required to eliminate 2*P* hub vertical shear, $t_c = 0.138$.

Table 1 Measured 2/rev hub vibration vs airspeed for a two-bladed teetering rotor[a]

Airspeed, kias	Fore-aft Amp, g	Fore-aft Phase,[b] deg	Lateral Amp, g	Lateral Phase, deg	Vertical Amp, g	Vertical Phase, deg
80	1.56	−24	1.47	−110	0.43	−161
100	2.04	−21	1.70	−113	0.83	−164
120	2.80	−34	2.47	−125	1.10	180
130	3.30	−34	2.94	−127	1.35	178
140	3.00	−35	2.73	−128	1.50	178

[a] Prototype model 222, ship 47001, flight 232A. [b] In two-per-rev space.

Table 2 Main rotor horsepower and 2*P* hub in-plane shears for a two-bladed teetering rotor, $\mu = 0.289$, $t_c = 0.138$

	M/R, hp	Longitudinal shear, lb	Lateral shear, lb
Baseline (without HHC)	657	661	596
HHC	730	920	870

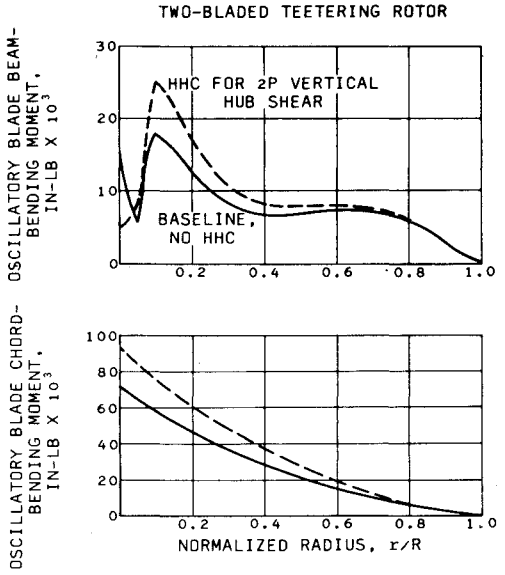

Fig. 3 Spanwise distribution of blade beam and chord oscillatory bending moments, $\mu = 0.289$, $t_c = 0.138$.

investigation was conducted to eliminate the 2*P* vertical shear using 2*P* collective inputs. The aircraft simulated was a prototype Bell Model 222—a two-bladed teetering rotor having a 2*P* nodal beam isolation system. The simulated gross weight was 7650 lb. The analytical procedure was first to compute performance, hub forces, and rotor loads at several airspeeds in level flight without implementing the HHC to obtain baseline forces. At an advance ratio of 0.289, a 1-deg amplitude 2*P* collective pitch was then imposed. Phase-shift angles of 0, 90, 180, and 270 deg were employed with the 1-deg amplitude. The 2*P* vertical forces with these harmonic pitches are shown in Fig. 1 as vectors. Also shown in Fig. 1 is the baseline force. The vectorial data shown in Fig. 1 indicate that a 2*P* collective pitch of a 2.7-deg amplitude and a 240-deg phase is required to cancel the 2*P* vertical force.

The same procedure was then repeated to an advance ratio of 0.192. A value of $\Delta\theta = 0.96$ deg $\cos(2\psi - 228$ deg) was used to null the 2*P* vertical shear. It is seen that the amplitude required to cancel the 2*P* vertical shear at $\mu = 0.192$ is smaller than that required at $\mu = 0.289$, and that the phase shift between the two advance ratios is quite small. Figure 2 depicts these observations.

Flight test measured 2*P* hub vibrations vs airspeeds for the prototype Model 222 having a nodal beam isolation system (and without HHC) are tabulated in Table 1. The data in Table 1 indicate that hub vibration levels increase with airspeed and are at nearly constant phase. Since the phase angles of the baseline configuration do not vary appreciably with airspeed, there is a good reason to believe that the HHC phase shift should be small with airspeeds, as was shown in Fig. 2.

The impact of HHC on rotor performance, hub in-plane forces, and rotor loads was also investigated. Data in Table 2 show comparisons of main rotor horsepower requirements, longitudinal and lateral hub shears with and without the 2*P* optimal collective pitch. The helicopter was trimmed in either flight simulation. As is shown, an 11% increase in main rotor horsepower was predicted using HHC due to blade stall in the fourth quadrant. The increases in hub in-plane shears demonstrate that the interharmonic coupling is strong and

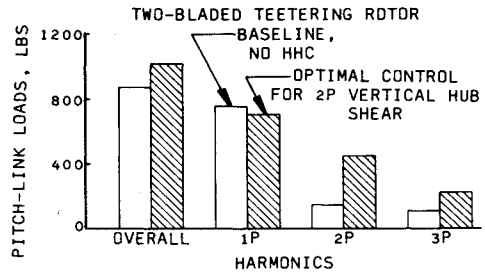

Fig. 4 Harmonic decomposition of pitch-link load at $\mu = 0.289$, $t_c = 0.138$.

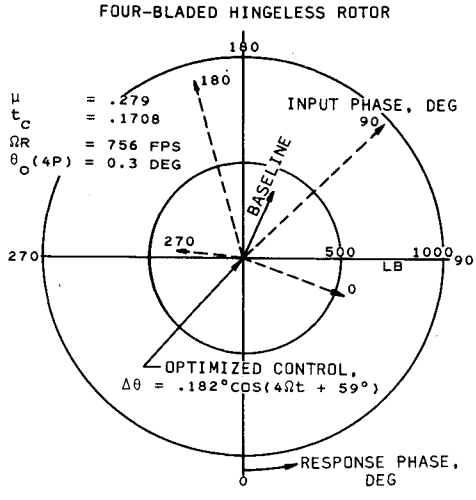

Fig. 5 Variation of 4*P* hub vertical shear with 4*P* collective input phase.

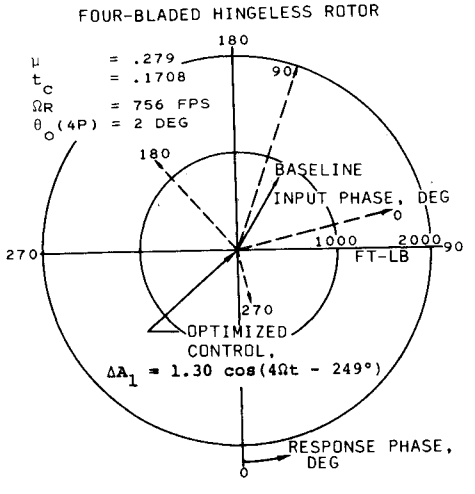

Fig. 6 Variation of 4*P* hub rolling moment with 4*P* lateral cyclic input phase.

that other HHC inputs would be required to simultaneously reduce all the hub shears.[3] However, use of collective HHC could only be advantageous because isolation of in-plane forces is mechanically simple and involves a small weight penalty.

Comparison of blade beam/chord-bending moments and pitch-link loads are given in Figs. 3 and 4, respectively. The oscillatory root beam-bending moment is lower using HHC at the expense of higher loads at the blade grip. The oscillatory root chord-bending moment was increased by 29% owing to HHC, and a 17% increase was predicted in the oscillatory pitch-link load. The increase in pitch-link load is mostly in the 2*P* component, as shown in Fig. 4.

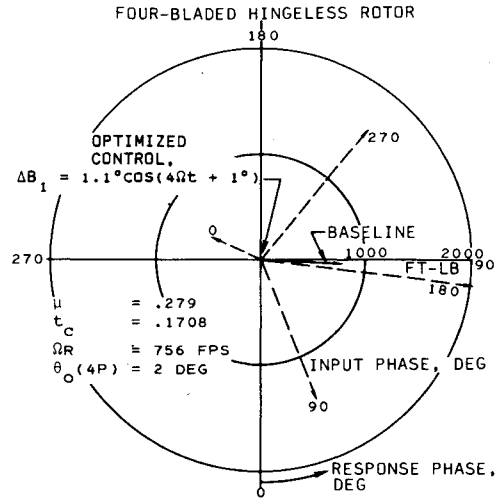

Fig. 7 Variation of 4*P* hub pitching moment with 4*P* longitudinal cyclic input phase.

Table 3 4*P* hub vertical force and moments calculated using inputs as a linear combination of optimal inputs for the respective single-input cases, $\mu = 0.279$, $t_c = 0.1708$

	Vertical shear, lb	Rolling moment, ft-lb	Pitching moment, ft-lb
Baseline	372 at 156 deg[a]	814 at 146 deg	706 at 80 deg
HHC	294 at 75 deg	366 at −166 deg	348 at 73 deg

[a] 372 at 156 = 372 cos (4Ω*t* − 156 deg).

Four-Bladed Hingeless Rotor HHC

Description of Math Model

C81 was also used in an investigation of HHC for a four-bladed hingeless rotor. The rotor was modeled using nine fully coupled elastic modes. Frequency of the first torsion mode was placed at 5.15*P*. The BUNS unsteady aerodynamics option was employed, and a higher-harmonic rotor wake model was used.[15] A complete fuselage dynamic and aerodynamic representation was math modeled for the rotorcraft in free flight.

Fixed System

Single input to the fixed system was made using 4*P* collective, 4*P* lateral swashplate tilt, as well as 4*P* longitudinal swashplate tilt. The analytical approach was very similar to that used for the teetering rotor: obtain a baseline, then impose a fixed amplitude 4*P* pitch, and vary its phase shift around the azimuth at 90-deg increments to derive the optimal control law using the vectorial data. The aircraft simulated was a prototype Bell Model 412—a four-bladed hingeless rotor with no vibration isolation system. The simulated gross weight was 11,500 lb. Results are presented in Figs. 5-7 for 4*P* collective, 4*P* lateral cyclic, and 4*P* longitudinal cyclic, respectively, at $\mu = 0.279$. The 4*P* vertical shear was reduced to zero with 0.182 deg of 4*P* pitch amplitude, while the rolling and pitching moments were nullified with 1.30-deg and 1.10-deg 4*P* swashplate tilting in the lateral and longitudinal directions, respectively. A linear combination of these optimal inputs was then imposed. The 4*P* vertical shear, rolling and pitching moments so obtained are compared with those for the baseline rotor in Table 3. Results indicate that there exists strong interharmonic couplings with HHC implemented in the fixed system.

This is not surprising and many discussions can be found in the literature describing techniques for deriving the required HHC for a multiple-input/multiple-output harmonic control. A numerical example for the flight condition simulated in this paper is given below, following the technique discussed in Ref. 11.

Table 4 Calculated hub loads from input phase 0 and 90 deg, $\mu = 0.279$, $t_c = 0.1708$[a]

Hub loads	Base-line	$\Delta\theta_c$, 0.3 deg/0	$\Delta\theta_s$, 0.3 deg/90	ΔB_{1c}, 2 deg/0	ΔB_{1s}, 2 deg/90	ΔA_{1c}, 2 deg/0	ΔA_{1s}, 2 deg/90
F_c	−341	180	−660	88	−1030	−177	−245
F_s	150	507	680	811	787	−1	423
PM_c	126	141	178	−182	1431	−498	190
PM_s	695	934	698	−545	354	667	25
RM_c	−677	−635	−605	−1190	−703	−348	−1849
RM_s	453	376	494	404	−80	1612	709

[a] Force in lb; moments in ft-lb.

At $\mu = 0.279$ and $t_c = 0.1708$, a $4P$ collective, $4P$ longitudinal cyclic, and $4P$ lateral cyclic with fixed amplitudes and 90-deg phase-shift increments were used as discussed in Figs. 5-7. A cosine feathering input was realized when the phase input was 0 deg and a sine feathering input was obtained when the phase input was 90 deg. The six hub-force components calculated from either of the six inputs (cosine and sine components of θ, B_1, and A_1) are tabulated in Table 4. Also shown are the baseline hub force and moments.

Assuming a general linear relationship between $4P$ hub responses and $4P$ feathering inputs, the following is defined[11]:

$$\Delta F_c = \frac{\partial F_c}{\partial \theta_c}\Delta\theta_c + \frac{\partial F_c}{\partial \theta_s}\Delta\theta_s + \frac{\partial F_c}{\partial B_{1c}}\Delta B_{1c} + \frac{\partial F_c}{\partial B_{1s}}\Delta B_{1s} + \frac{\partial F_c}{\partial A_{1c}}\Delta A_{1c} + \frac{\partial F_c}{\partial A_{1s}}\Delta A_{1s} \tag{1}$$

The same expression can be written for other hub response components. In matrix notation,

$$\begin{bmatrix} \Delta F_c \\ \Delta F_s \\ \Delta P_c \\ \Delta P_s \\ \Delta R_c \\ \Delta R_s \end{bmatrix} = [T] \begin{bmatrix} \Delta\theta_c \\ \Delta\theta_s \\ \Delta B_{1c} \\ \Delta B_{1s} \\ \Delta A_{1c} \\ \Delta A_{1s} \end{bmatrix} \tag{2}$$

Using the data in Table 4, the transfer matrix $[T]$ was calculated.

$$[T] = \begin{bmatrix} 1736.6 & -1063.3 & 214.5 & -344.5 & 82.0 & 48.0 \\ 1190.0 & 1766.6 & 330.5 & 318.5 & -75.5 & 136.5 \\ 50.0 & 173.3 & -154.0 & 652.5 & -312.0 & 32.0 \\ -203.3 & 10.0 & -620.0 & -170.5 & -14.0 & -335.0 \\ 140.0 & 240.0 & -256.5 & -13.0 & 164.50 & -586.0 \\ -256.6 & 136.6 & -24.5 & -266.5 & 579.5 & 128.0 \end{bmatrix} \tag{3}$$

The swashplate multiple inputs to null vibration were solved by investing the transfer matrix and performing the following calculations:

$$\begin{bmatrix} \Delta\theta_c \\ \Delta\theta_s \\ \Delta B_{1c} \\ \Delta B_{1s} \\ \Delta A_{1c} \\ \Delta A_{1s} \end{bmatrix} = [T]^{-1} \begin{bmatrix} 341 \\ -150 \\ -126 \\ -695 \\ 677 \\ -453 \end{bmatrix} \tag{4}$$

The results are

collective: $0.367\cos(4\Omega t + 108 \text{ deg})$ (5a)

longitudinal cyclic: $2.293\cos(4\Omega t - 15.2 \text{ deg})$ (5b)

lateral cyclic: $2.277\cos(4\Omega t + 86.9 \text{ deg})$ (5c)

It is noticed that the amplitudes of the optimal pitch angles nearly doubled those required for the single-input cases (Figs. 5-7).

The pitch angles, shown in Eq. (5), were then used in the analysis. The calculated hub responses with these inputs indicate a 65% reduction in the hub vertical shear, 84% reduction in the pitching moment, and 80% reduction in the rolling moment. Failure to completely eliminate the hub forces indicates nonlinearities in the system. To investigate the degree of nonlinearity, a new transfer matrix was formed by perturbating each of the six feathering inputs. The perturbated feathering inputs were obtained by inverting the new transfer matrix. The HHC inputs were then updated by adding the perturbated values to the previous HHC [Eq. (5)].

The updated HHC inputs are

collective: $0.356\cos(4\Omega t + 111.5 \text{ deg})$ (6a)

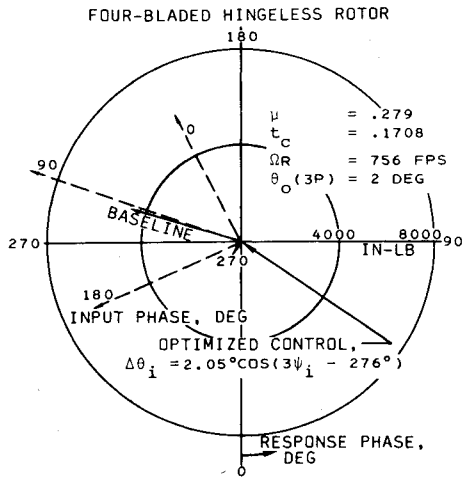

Fig. 8 Variation of 3*P* blade root beam-bending moment with 3*P* pitch phase in rotating system.

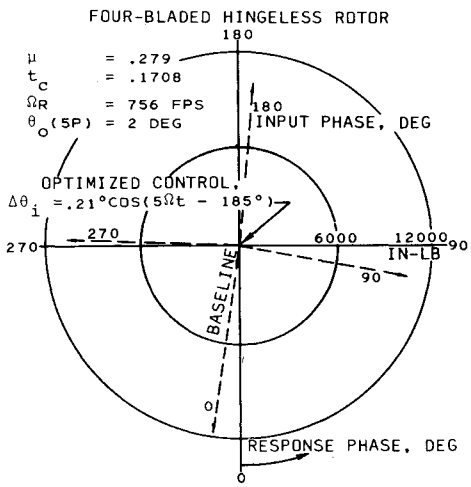

Fig. 9 Variation of 5*P* blade root beam-bending moment with 5*P* pitch phase in rotating system.

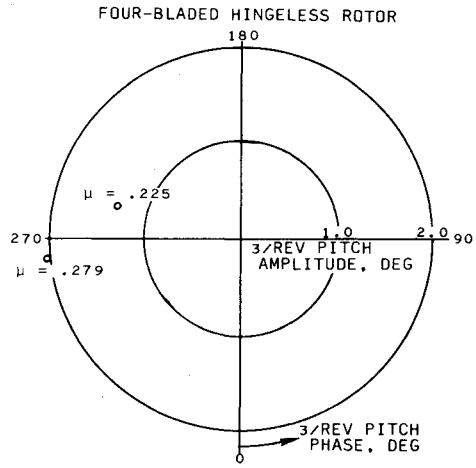

Fig. 10 Effect of advance ratio on 3*P* pitch required to eliminate 3*P* blade root beam-bending moment, $t_c = 0.17$.

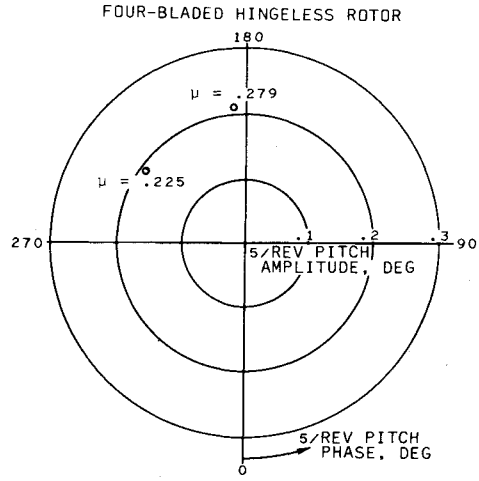

Fig. 11 Effect of advance ratio on 5*P* pitch required to eliminate 5*P* blade root beam-bending moment, $t_c = 0.17$.

longitudinal cyclic: $2.187\cos(4\Omega t - 10.4 \text{ deg})$ (6b)

lateral cyclic: $2.133\cos(4\Omega t + 87.6 \text{ deg})$ (6c)

Hub responses obtained using the current HHC [in Eq. (6)] indicate an 80% reduction in the vertical shear and nearly a complete elimination of the moments. Since there is still a 20% vertical shear to minimize, additional iterations are required for a complete elimination of all of the hub responses.

It is interesting to repeat the preceding computation procedure when the phase inputs of 180 and 270 deg were used to form the data array similar to those tabulated in Table 4. The optimal HHC inputs thus calculated are

θ: $0.278\cos(4\Omega t + 132 \text{ deg})$ (7a)

B_1: $1.982\cos(4\Omega t - 9.1 \text{ deg})$ (7b)

A_1: $2.0\cos(4\Omega t + 95 \text{ deg})$ (7c)

Comparisons of the HHC in Eq. (7) with those in Eq. (5) reveal noticeable differences. These differences and the fact that an iterative procedure was required to achieve an absolute minimum suggest that the elements of the transfer matrix are dependent upon the HHC themselves. Therefore the relationship between the HHC input and the hub response for a simultaneous elimination of the shear and the moments is apparently nonlinear.

Rotating System

Since the 4*P* hub rolling and pitching moments originate from blade root 3*P* and 5*P* beam-bending moments, studies were made to minimize hub moments using HHC in the rotating system. The results are presented in Figs. 8-11. Data in Figs. 8 and 9 indicate that an amplitude of 2.05 deg of 3*P* pitch is required to optimize the blade root 3*P* beam-bending moment, and that 0.21 deg is required to optimize the 5*P* component.

Effect of advance ratio on phase angles for 3*P* and 5*P* feathering in the rotating system and 4*P* collective oscillation in the fixed system is shown in Figs. 10-12, respectively. As indicated, phase shift due to advance ratio is quite large in all these cases.

Table 5 validates the above analytical findings. Flight test data, as presented in Table 5, indicate that variation in phase angles of 4*P* vertical shear, blade root 3*P*, and 5*P* beam moments with airspeed can be quite large.

A linear combination of the optimal control found in Figs. 5, 8, and 9 was then begun. It was found that the influence of the interharmonic coupling was not so great in collective/rotating-system harmonic-pitch-control as that in collective/swashplate tilting. Only a small adjustment in 4*P* collective pitch was required to achieve complete cancellation of 4*P* vertical shear and nearly 90% reduction in both 4*P* rolling and pitching moments. The effect of this HHC on rotor performance and 4*P* hub in-plane shears, oscillatory

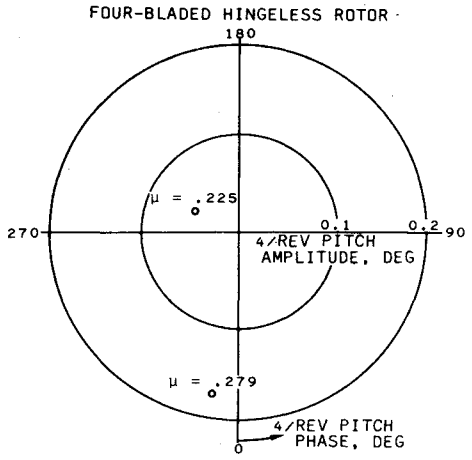

Fig. 12 Effect of advance ratio on 4*P* pitch required to eliminate 4*P* hub vertical shear, $t_c = 0.17$.

Table 5 Measured 4*P* hub vertical vibration and blade 3*P* and 5*P* yoke-beam-bending moments vs airspeeds for a four-bladed hingeless rotor[a]

Airspeed, kias	4*P* hub vertical Amp, g	Phase,[b] deg	Yoke-beam 3*P* Amp, in.-lb	Phase, deg	Yoke-beam 5*P* Amp, in.-lb	Phase, deg
20	0.23	−119	609	−21	474	151
60	0.06	125	646	119	324	96
80	0.11	99	921	146	380	110
100	0.18	99	1359	160	479	125
120	0.28	148	1965	−163	819	153
130	0.28	163	2214	−150	907	138

[a] Prototype model 412, ship 20963, flight 9A. [b] In *N*-per-rev space, e.g., amp•cos ($N\Omega t$ − phase).

Table 6 *M/R* hp and 4*P* hub in-plane shears for a four-bladed hingeless rotor, $\mu = 0.279$, $t_c = 0.1708$

	M/R, hp	Longitudinal shear, lb	Lateral shear, lb
Baseline (without HHC)	1018	296	291
HHC[a]	1046	54	103

[a] 3*P*, 4*P*, and 5*P*.

blade beam moments, and pitch-link loads is presented in Table 6 and Figs. 13 and 14, respectively. An increase in main rotor horsepower of 2.7% was predicted owing to HHC. (A force-moment trim was achieved for both conditions.) The 4*P* hub in-plane shears and blade beam moments are generally lower with HHC. The blade chord bending was not affected (not shown) by the HHC. The oscillatory pitch-link load was increased by 16% using HHC with the most increase in the 3*P* harmonic component.

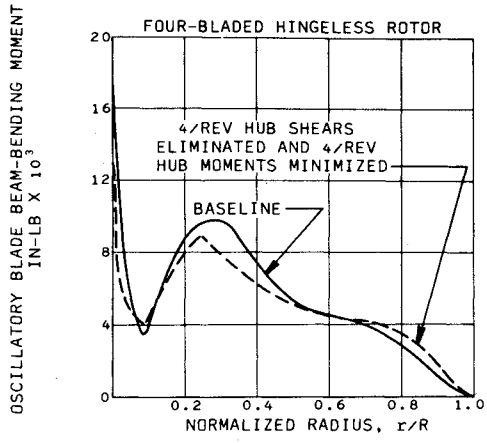

Fig. 13 Effect of simultaneous elimination of 4*P* hub vertical shear, rolling and pitching moments using HHC in blade rotating system, $\mu = 0.279$ and $t_c = 0.1708$.

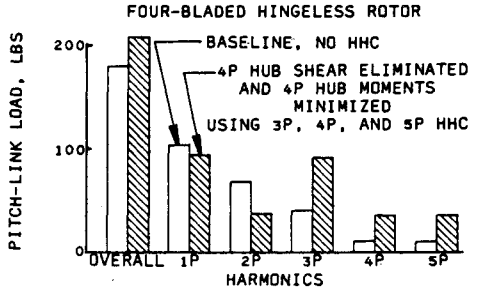

Fig. 14 Harmonic decomposition of pitch-link load at $\mu = 0.279$ and $t_c = 0.1708$.

References

[1] Wernicke, R.K. and Drees, J. M., "Second Harmonic Control," *Proceedings of the American Helicopter Society, Inc.*, 19th Annual National Forum, Washington, D.C., May 1963, pp. 1-7.

[2] Daughaday, H., "Suppression of Transmitted Harmonic Rotor Loads by Blade Pitch Control," USAAVLABS TR 67-14, Nov. 1967.

[3] Balcerak, J.C. and Erickson, J.C. Jr., "Suppression of Transmitted Harmonic Vertical and In-plane Rotor Loads by Blade Pitch Control," USAAVLABS TR-69-39, July 1969.

[4] McCloud, J.L. III, "An Analytical Study of a Multicyclic Controllable Twist Rotor," AHS Preprint No. 932, presented at the 31st Annual National Forum of American Helicopter Society, Washington, D.C., May 1975.

[5] Shaw, J. Jr., "Higher-Harmonic Blade Pitch Control for Helicopter Vibration Reduction: A Feasibility Study," ASRL TR 150-1, Aeroelastic and Structures Research Laboratory, M.I.T., Dec. 1968.

[6] London, R.J., Watts, G.A., and Sissingh, G. J., "Experimental Hingeless Rotor Characteristics at Low Advance Ratio with Thrust," NASA CR-114684, Dec. 1973.

[7] Sissingh, G.J. and Donham, R.E., "Hingeless Rotor Theory and Experiment on Vibration Reduction by Periodic Variation of Conventional Controls," presented at the AHS/NASA-Ames Specialists' Meeting on Rotorcraft Dynamics, Feb. 1974.

[8] McHugh, F.J. and Shaw, J. Jr., "Benefits of Higher-Harmonic Blade Pitch: Vibration Reduction, Blade-Load Reduction and Performance Improvement," presented at the American Helicopter Society Mideast Region Symposium on Rotor Technology, Aug. 197

[9] McHugh, F.J. and Shaw, J. Jr., "Helicopter Vibration Reduction with Higher-Harmonic Blade Pitch," presented at the Third European Rotorcraft and Powered-Lift Aircraft Forum, Aix-en-Provence, France, Sept. 1977.

[10] Hammond, C.E., "Helicopter Vibration Reduction Via Higher Harmonic Control," Structures Laboratory, U.S. Army Research and Technology Laboratories, *Proceedings of the Rotorcraft Vibration Workshop,* NASA Ames Research Center, Feb. 1978.

[11] Wood, E.R., Powers, R.W., and Hammond, C.E., "On Methods for Application of Harmonic Control," presented at the Fourth European Rotorcraft and Powered-Lift Aircraft Forum, Stresa, Italy, Sept. 1978.

[12] Powers, R.W., "Application of Higher Harmonic Blade Feathering for Helicopter Vibration Reduction," submitted to the Western Region of the AHS in competition for the Robert L. Lichten Award, 1979.

[13] McLarty, T.T., "Rotorcraft Flight Simulation with Coupled Rotor Aeroelastic Stability Analysis," USAAMRDL TR 76-41A, May 1977.

[14] Sadler, S.G., "Documentation of Myklestad Analysis (DNAM06)," Bell Helicopter Textron Rept. No. 299099-608, Oct. 1979.

[15] Sadler, S.G., "Development and Application of a Method for Predicting Rotor Free Wake Positions and Resulting Rotor Blade Air Loads, Vol. I—Model and Results," NASA CR-1911, Dec. 1971.